International Journal of Hygiene and Environmental Health 222 (2019) 1115–1132

Contents lists available at ScienceDirect

International Journal of Hygiene and Environmental Health

journal homepage: www.elsevier.com/locate/ijheh

Effects of short-term exposure to fine and ultrafine particles from indoor sources on arterial stiffness – A randomized sham-controlled exposure study

Vanessa J. Soppa[a,*], Samir Shinnawi[a], Frauke Hennig[a], Birgitta Sasse[a], Bryan Hellack[b,c], Heinz Kaminski[c], Ulrich Quass[d], Roel P.F. Schins[e], Thomas A.J. Kuhlbusch[f,g], Barbara Hoffmann[a]

[a] Institute for Occupational, Social and Environmental Medicine, Center for Health and Society, Heinrich Heine University of Düsseldorf, 40225, Düsseldorf, Germany
[b] Federal Environment Agency of Germany, Paul-Ehrlich-Str. 29, 63225, Langen, Germany
[c] Institute of Energy and Environmental Technology (IUTA) e.V., 47229, Duisburg, Germany
[d] LANUV - Landesamt für Natur, Umwelt und Verbraucherschutz Nordrhein-Westfalen Fachbereich 44, 45133, Essen, Germany
[e] IUF-Leibniz Research Institute for Environmental Medicine, 40225, Düsseldorf, Germany
[f] Federal Institute for Occupational Safety and Health (BAuA), 44149, Dortmund, Germany
[g] CENIDE - Center for Nanointegration, 47057, Duisburg, Germany

ARTICLE INFO

Keywords:
Fine and ultrafine indoor particles
Arterial stiffness
Pulse wave analysis
Controlled exposure

ABSTRACT

Objectives: Particulate air pollution is linked to adverse cardiovascular effects, including arterial stiffness. The aim of the study was to investigate the effect of short-term exposure to indoor fine and ultrafine particles on augmentation index (AIx), augmentation pressure (AP), and pulse wave velocity (PWV), early signs of vascular damage.

Methods: We analyzed the association of particle emissions from typical indoor sources (candle burning - CB, toasting bread - TB, and frying sausages - FS) with changes in pulse wave analysis indices in 55 healthy adults in a randomized cross-over controlled exposure study. Particle mass concentration (PMC), size-specific particle number concentration (PNC) and lung-deposited particle surface area concentration (PSC) were measured during the 2 h exposure. AIx and AP were measured before, directly, 2, 4 and 24 h after exposure. PWV was measured directly and 24 h after exposure. We performed multiple mixed linear regression analyses of different particle metrics and AIx, AP and PWV.

Results: The highest mean PMC was observed during FS reaching a maximum of 210 $\mu g/m^3$ PM_{10}. The maximal PNC for UFP < 100 nm was reached during CB with 2.3 million particles/cm^3. PSC was similar across all three exposures (about 3000 $\mu m^2/cm^3$). Strongest associations between different particles metrics and arterial stiffness indices could be observed for UFP from CB and FS and for PMC from TB. The highest mean increase could be observed for the UFP fraction < 10 nm, measured during CB, and AIx with an increase of 9.5%-points (95%-CI: 3.1; 15.9). PSC seemed to follow the pattern of PNC. PM_{10} and $PM_{2.5}$ from TB led to clear changes in AIx with biggest increases for PM_{10} of 5.8%-points (95%-CI: 3.2; 8.4) 2 h after exposure and for $PM_{2.5}$ of 8.1%-points (95%-CI: 2.5; 13.7) directly after exposure.

Conclusions: Our study indicates effects of indoor exposure to fine and ultrafine particles on systemic arterial stiffness indices that depend on the indoor source as well as on particle metric. Differences in size-specific physical characteristics of source-specific particles might account for these differential effects. We did not observe clear and stable associations of indoor particle exposure and PWV.

1. Introduction

Exposure to ambient particulate matter (PM) is a leading cause of global morbidity and mortality (Lim‡ et al., 2012). Epidemiological Studies have confirmed the association between air pollution and adverse cardiovascular health effects (Brook et al., 2010) (Cesaroni et al., 2014). Additionally, air pollution has been linked to arterial stiffness (AS) (Mehta et al., 2014) which in turn seems to be a risk factor for

* Corresponding author.
E-mail addresses: vanessa.soppa@uni-duesseldorf.de (V.J. Soppa), samir.shinnawi@uni-duesseldorf.de (S. Shinnawi), frauke.hennig@uni-duesseldorf.de (F. Hennig), birgitta.sasse@uni-duesseldorf.de (B. Sasse), bryan.hellack@uba.de (B. Hellack), kaminski@iuta.de (H. Kaminski), Ulrich.Quass@lanuv.nrw.de (U. Quass), roel.schins@IUF-Duesseldorf.de (R.P.F. Schins), Kuhlbusch.Thomas@baua.bund.de (T.A.J. Kuhlbusch), b.hoffmann@uni-duesseldorf.de (B. Hoffmann).

https://doi.org/10.1016/j.ijheh.2019.08.002
Received 24 January 2019; Received in revised form 13 July 2019; Accepted 6 August 2019
1438-4639/

cardiovascular (CV) disease, independent of other risk factors (Veerasamy et al., 2014). Stiffness of elastic arteries like the aorta is an independent predictor of all-cause mortality and has been linked to increased mortality, especially CV mortality, in patients with uncomplicated hypertension (Laurent et al., 2001), diabetes mellitus type 2 (Cruickshank et al., 2002), end-stage renal disease (Shoji et al., 2001), older individuals (Steppan et al., 2011) and even in the general population (Willum-Hansen et al., 2006).

One important fraction of ambient particles are UFPs, here defined as particles with electrical mobility diameters below 100 nm. High PNC, their increased specific surface area and their oxidative potential compared to larger particles at the same mass concentration are discussed to be relevant parameters determining their pathogenic potential (Brown et al., 2001; HEI Review Panel on Ultrafine Particles, 2013; Li et al., 2003; Oberdorster et al., 1995). They furthermore have a very high predicted deposition efficiency in the pulmonary region, can reach the alveolar space, penetrate the epithelium and might gain access to the pulmonary interstitium and systemic circulation (HEI Review Panel on Ultrafine Particles, 2013; Kapp et al., 2004; Miller et al., 2017). In the most recent review, strongest evidence was observed for short-term exposure to UFP and pulmonary and systemic inflammation, blood pressure and heart rate variability (Ohlwein et al., 2019().

In urban areas, diesel or biomass combustion processes are the mayor source of UFP. High number concentration at these sources combined with fast agglomeration and dilution processes lead to steep concentration gradients with increasing distance from the source (Karner et al., 2010). Diesel exhaust and wood smoke, which are rich in UFPs, have been shown to be related to increases in arterial stiffness and pulse wave velocity (PWV) (Lundback et al., 2009; Unosson et al., 2013). However, little evidence is available on the effects of exposure to inhalable particles from indoor sources, that emit substantial amounts of fine and UFPs (Afshari et al., 2005), leading to high exposure levels (Brasche and Bischof, 2005; Ghio et al., 2012; Sørensen et al., 2005; Ward and Noonan, 2008) and high cumulative exposures due to the length of time spent indoors. In our previous publication we found first evidence that short-term exposure to UFP from common indoor sources is associated with increases in blood pressure (Soppa et al., 2017). Arterial stiffness predates essential hypertension and has an impact on the coronary flow reserve even in mild coronary artery disease (Veerasamy et al., 2014). Based on our prior work, we focused on further cardiovascular outcomes to substantiate the toxicity of indoor air pollutants and shed more light on the underlying biological mechanisms.

For this purpose we investigated whether exposure to particles generated from candle burning (CB), frying sausages (FS) and toasting bread (TB) leads to changes in arterial stiffness in healthy adults in a cross-over sham-controlled exposure study. We investigated the role of different particle metrics (particle mass concentration - PMC, particle surface concentration - PSC and particle number concentration - PNC), paying special attention to the UFPs by analyzing the effects of different particle size fractions of UFPs.

2. Material and methods

The “Effects of fine and ultrafine Particles from Indoor Activities” (EPIA) project is a cross-over sham-controlled exposure study with healthy adults, which integrates a detailed exposure characterization, the investigation of biological pathways with toxicological methods, and human health effect analyses. It was approved by the Ethics Committee of the Heinrich-Heine-University of Düsseldorf, in accordance with the declaration of Helsinki. All participants gave written informed consent.

The study protocol has been described in detail elsewhere (Soppa et al., 2014). In short, 55 adult men and women were recruited for this study. Inclusion criteria comprised age between 18 and 79 years, speaking and understanding German, and being a non-smoker or ex-smoker for at least ten years. All subjects were asked to abstain from alcohol and extreme physical exercise for 24 h and from caffeine drinks for at least 4 h before the beginning of each exposure. On the morning of the exposure days participants obtained only a light breakfast of pre-described food. If a participant had a current infection or had taken anti-inflammatory drugs during the previous seven days, the exposure was rescheduled. On average four participants were exposed on each exposure day.

Each exposure session lasted for 2 h and took place in an air-conditioned custom-made laboratory room. The air conditioning system worked in a circulating mode, hence not causing additional air exchange. Air flow rate was approximately 240 m^3/h. During exposure, temperature (24 °C) and relative humidity were controlled. Participants were exposed on separate occasions at the same time of day at least two weeks apart. The order of the exposure sessions was randomized. Participants were not blinded against the type of exposure because the particle sources were placed inside the exposure chamber so that the subjects could see them and smell source-specific odours. For the sham exposure with room air (RA), an air refresher (out of operation) was placed in the chamber to mimic a further exposure scenario. Participants were sitting during exposure sessions so breathing patterns corresponded to usual resting indoor activities.

In the experimental exposure scenarios, participants were exposed to CB, TB and FS on two different exposure levels (low and high exposure). Indoor sources were operated by staff members, present continuously inside the chamber.

PNC and PSC in the exposure chamber were monitored continuously during each session to ensure consistent particle exposure levels for all participants and each exposure scenario as well as to calculate the individual 2 h particle exposure for each participant and exposure condition. Fluctuation of concentrations, for example, due to opening the exposure room door was thus included in the personalized cumulative exposure. Before a subject entered the exposure chamber the sources had already been activated for at least 30 min to ensure that the particle concentration reached an equilibrium. Size-specific number concentration of particles from 5.6 nm to 560 nm size range was monitored by a Fast Mobility Particle Sizer (FMPS, Model 3091, TSI Inc., Shoreview, MN, USA) and for particles from 0.6 µm to 20 µm with an Aerodynamic Particle Sizer (APS, Model 3321, TSI Inc.). Further, the alveolar deposited surface area particle concentration was monitored using a Nanoparticle Surface Area Monitor (NSAM, Model 3550, TSI Inc.). Additionally, size-specific mass concentrations of PM_1, $PM_{2.5}$ and PM_{10} were calculated from particle size and number concentrations assuming spherical particles and a particle density of 1 g/cm^3. A High-Resolution Time-of-Flight Aerosol Mass Spectrometry enabled a continuous (once per second) acquisition of complete mass spectra of individual particles with aerodynamic diameter of 60–600 nm, and enabled the resolution of distinct chemical species based on mass defect. Additional information on the particle characteristics were gained during prior exposure scenario measurements without participants. For the UFPs a Nanometer Aerosol Sampler (NAS) was used to create samples of the aerosols charging them onto a substrate. This substrate was removed and examined using a Total Reflection X-ray Fluorescence (TXRF) to characterize the elemental composition of the ultrafine fraction. In addition an organic carbon and elemental carbon (OC-EC) aerosol analysis was conducted with the Sunset OC-EC Analyzer from samples sampled on quartz fiber filters.

Ambient air pollution data ($PM_{2.5}$ concentrations) were obtained from the State Agency for Nature, Environment and Consumer Protection in North Rhine Westphalia (LANUV), referring to the nearest monitoring station to the home of the participants. A more detailed description of the study protocol and particle measurements, including device names, can be found in Soppa et al. (2017).

All pulse wave measurements were taken by trained technicians in quiet and well-tempered conditions within the study center using the SphygmoCor® System (CPV; AtCor Medical, Sydney, Australia). For the

International Journal of Hygiene and Environmental Health 222 (2019) 1115–1132

assessment of arterial stiffness we conducted a PWA and measured Pulse Wave velocity (PWV). Even though the gold standard of measuring the PWV is the derivation from the carotid artery and femoral artery, we decided to deduce the pulse wave at the carotid artery and radialis artery, because of practical reasons (Baulmann et al., 2010). As additional potential predictors for arterial stiffness we performed a PWA measuring the Augmentation Index (AIx) and the Augmentation Pressure (AP). We measured the AIx and the AP at five different time points: pre exposure, directly after, and 2 h, 4 h, and 24 h after exposure. The SphygmoCor® pulse wave analysis option provides a derived ascending aortic blood pressure waveform and a range of central arterial indices. The standard operating procedure (SOP) used in this study was as follows: Each pulse wave analysis was performed at least 2 min after the brachial blood pressure measurement to enable the radial arterial to refill with blood. Thus, before starting the PWA, participants rested in a relaxed position for at least 15 min. The pressure transducer (tonometer) was placed over the strongest pulse point of the radial artery. The tonometer was kept in this position saving reproducible waveforms for the analysis. In order to get high quality data, we followed the quality control parameters from the AtCor research application manual (AtCor Medical Pty. Ltd., 2010). The following quality criteria had to be met for each measurement: average pulse height ≥80, pulse height variation ≤5%, diastolic variation ≤5%, shape deviation ≤4, and operator index > 80%. The results for AIx and AP are presented normalized to 75 heart beats per minute for better comparability.

Pulse wave velocity was measured pre-exposure, directly after, and 24 h after exposure, each directly after the pulse wave analysis. A total of three electrodes were attached to the lying subjects left and right arm and left leg. At first the tonometer was placed over the strongest pulse point of the right carotid arteria. The tonometer was kept in this position until reproducible waveforms for the analysis could be recorded. The second measurement was carried out in the same way at the strongest pulse point of the radial artery. One essential quality criteria that had to be met was standard deviation of the mean PWV under 10%.

3. Statistical analysis

The exposure data, used in the following analyses, is composed of the particle concentration measured during CB, FS, and TB in level 1 and level 2. Because of the substantial overlap of exposure concentrations at level 1 and level 2 we analyzed the data as the actual measured exposure concentration. To analyze exposure source-related changes on pulse wave indices, we performed multiple mixed linear regression analyses with a random participant intercept, including an indicator for each exposure source (room air as reference) and the intra-individual difference of AIx, AP and PWV at time point t_n compared to the corresponding values taken before the exposure (t_0) as the dependent variables. Each time point was analyzed in a separate regression model (Soppa et al., 2017). Covariates in the full model included age, height, weight, sex, mean temperature and humidity in the chamber, travel time to the study location before exposure, mode of transportation and ambient $PM_{2.5}$ concentration, averaged over the last five days before the study day.

In a second analysis step, we examined the time-dependent impact of mean personal exposure on changes in AIx, AP, and PWV by including indicator variables for time point and interaction terms for time point*exposure metric. Because of possible source-specific effects of the three particle sources on AIx, AP, and PWV, we conducted separate models for each exposure (CB, TB and FS).

For the comparison of the effect of different particle metrics (PMC, PSC and PNC) within one source, we calculated the changes in AIx, AP, and PWV per interquartile range (IQR). A corresponding table with the information on the IQR can be found in the appendix (Table A2). Additionally we calculated the effects of different size fractions of UFPs (< 10 nm, 10–30 nm, 30–50 nm, 50–100 nm) on AIx, AP, and PWV within one source. In order to detect possible independent effects of PNC and PMC measured during CB, FS and TB on arterial stiffness, we additionally adjusted PNC exposures for PM_{10} and PMC exposures for UFP in separate analyses of two-pollutant models. A correlation table, showing the correlation coefficient (Spearman r) between exposure metrics (PMC, PSC, PNC) at different exposure scenarios (RA, CB, TB, FS) was calculated and is attached in the appendix (Table A1).

Statistical analyses were performed using SAS version 9.2 (SAS/STAT Software, SAS Institute, Inc., Cary, NC, USA) and RStudio (R 3.2.5, Development Core Team, Vienna, Austria).

Table 1
Personal characteristics of the study population (N = 55) at their first study center visit, unless otherwise stated. EPIA Study, Germany (September 2012–April 2013).

Personal Characteristic	Measure
Age [years], mean (SD)	32.5 (16.3)
Born in Germany, n (%)	35 (65.0)
Height [cm], mean (SD)	173.9 (9.4)
Weight [kg], mean (SD)	71.7 (13.3)
Male, n (%)	27 (49.0)
BMI [kg/m[b]], mean (SD)	23.6 (3.2)
Baseline blood pressure (N = 255)[a]	
Systolic [mmHg], mean (SD)	116.0 (13.8)
Diastolic [mmHg], mean (SD)	74.8 (9.7)
Controlled hypertension, n (%)	2 (3.7)
Baseline central arterial indices (N = 255)[a]	
Augmentation pressure [mmHg], mean (SD)	2.4 (4.2)
Augmentation index [%], mean (SD)	8.1 (13.1)
Pulse wave velocity [m/s], mean (SD)	7.5 (1.6)
Smoking status, n (%)	
Ex-smoker	3 (5.4)
Never-smoker	51 (92.7)
Missing	1 (1.9)
Level of education, n (%)	
Low	4 (7.3)
Medium	5 (9.1)
High	42 (76.3)
Missing	4 (7.3)
Employed, n (%)	26 (49.0)
Means of transportation, n (%) (N = 255)[b]	
Car	102 (39.8)
Public transport	143 (56.3)
Missing	10 (3.9)
Travel time, hours, mean (SD)	1.1 (0.6)

[a] Mean value calculated from the pre exposure measurements (per participant and exposure).
[b] Used means of transportation per participant and exposure.

4. Results

4.1. Study population

Altogether, 55 participants were included in this study, with 27 males and 28 females and an average age of 32.5 years (Table 1). Participants completed on average 4.6 exposure sessions, resulting in an average of 27.8 valid pulse wave analysis measurements per participant. Baseline AP and AIx was 2.4 ± 4.2 mmHg and 8.1 ± 13.1%. Baseline PWV was 7.5 ± 1.6 m/s.

4.2. Exposure

Each participant underwent one control exposure and up to six experimental exposures. The N's shown in Table 2 pertain to the number of observations available for each exposure. The maximum UFP number concentration (< 100 nm) was observed during CB with 2,311,085 ± 449,555 #/cm^3 (Table 2). The highest mean mass concentration was determined during FS reaching a maximum of 211.0 ± 145.6 µg/m^3 for PM_{10}. Mean PSC did not differ clearly

Table 2
Description of personal 2 h means and standard deviations of different particle metrics: PMC (PM_{10}, $PM_{2.5}$ and PM_1), PNC (*10^3) (< 10 nm, 13–30 nm, 30–50 nm, 50–100 nm, < 100 nm) and PSC during room air (RA), candle burning (CB), toasting bread (TB) and frying sausages (FS).

Particle metric	N	Mean ± SD	Min	Max	Q1	Median	Q3
Room air							
PMC [µg/m³]							
PM_{10}	34	6.3 ± 5.8	2.4	30.2	3.7	4.3	5.4
$PM_{2.5}$	34	4.8 ± 5.4	1.5	26.8	2.5	3.1	3.6
PM_1	34	3.3 ± 3.6	0.9	16.8	1.3	2.2	2.6
PSC [µm²/cm³]	46	22.9 ± 18.0	7.5	75.6	13.7	17.5	20.6
PNC [#/cm³]							
< 10 nm	46	0.2 ± 0.3	0.0	0.9	0.0	0.2	0.3
10–30 nm	46	1.0 ± 0.8	0.4	4.4	0.5	0.8	1.1
30–50 nm	46	0.9 ± 0.7	0.3	3.4	0.5	0.7	1.0
50–100 nm	46	1.3 ± 1.1	0.4	4.8	0.7	0.9	1.2
< 100 nm	46	3.4 ± 2.1	1.3	9.9	1.8	3.0	4.2
Candle burning							
PMC [µg/m³]							
PM_{10}	61	72.6 ± 20.4	30.9	108.2	56.3	77.0	87.4
$PM_{2.5}$	61	69.6 ± 19.9	29.7	105.4	51.6	74.7	84.4
PM_1	61	66.8 ± 20.3	28.1	100.1	49.4	67.5	83.3
PSC [µm²/cm³]	72	3034.5 ± 918.9	1211.6	4675.9	2339.9	2908.6	3728.5
PNC [#/cm³]							
< 10 nm	72	359 ± 97	79	509	283	378	432
10–30 nm	72	1387 ± 250	744	1818	1168	1368	1577
30–50 nm	72	425 ± 103	261	619	327	425	496
50–100 nm	72	138 ± 66	52	289	86	125	180
< 100 nm	72	2311 ± 449	1144	3064	1863	2434	2669
Toasting bread							
PMC [µg/m³]							
PM_{10}	59	73.0 ± 53.5	19.9	396.5	40.0	69.0	93.5
$PM_{2.5}$	59	65.0 ± 31.4	18.6	159.9	37.8	65.1	88.7
PM_1	59	60.7 ± 28.9	17.1	157.1	36.3	61.6	81.3
PSC [µm²/cm³]	66	2776.7 ± 1144.2	1203.0	5144.1	1829.4	2568.6	3659.4
PNC [#/cm³]							
< 10 nm	65	76 ± 16	47	109	61	72	92
10–30 nm	65	561 ± 117	362	745	464	526	664
30–50 nm	65	404 ± 139	172	672	292	414	504
50–100 nm	65	198 ± 104	48	448	112	201	278
< 100 nm	65	1240 ± 361	669	1884	919	1233	1521
Frying sausages							
PMC [µg/m³]							
PM_{10}	64	211.0 ± 145.6	26.1	547.4	66.6	210.3	324.5
$PM_{2.5}$	64	169.3 ± 110.2	24.5	401.1	54.4	178.3	244.5
PM_1	64	148.4 ± 99.2	21.8	384.3	47.6	149.1	209.7
PSC [µm²/cm³]	70	2416.8 ± 1469.3	612.8	5538.3	1054.1	2195.1	3647.1
PNC [#/cm³]							
< 10 nm	70	5 ± 3	1	13	3	4	7
10–30 nm	70	82 ± 25	44	132	63	76	105
30–50 nm	70	156 ± 59	72	280	109	144	186
50–100 nm	70	216 ± 126	39	452	98	206	315
< 100 nm	70	461 ± 177	199	824	310	418	596

between the exposure scenarios (CB: 3034.5 ± 918.9 µm²/cm³; TB: 2776.7 ± 1144.2 µm²/cm³; FS: 2416.8 ± 1469.3 µm²/cm³) (Table 2). During CB, the UFP concentration was dominated by particles between 10 and 30 nm, during TB by particles between 10 and 50 nm and during FS by particles between 50 and 100 nm. Correlations between PM_{10} and UFP number concentration measured during CB, TB and FS were low to mostly moderate (r: 0.54 to 0.84) (Table A1).

4.3. Exposure-outcome associations

When investigating whether exposure to particles from CB, FS and TB led to changes in arterial stiffness we conducted an overall comparison of exposure sources (categorical model 1). We observed a small and transient increase in AP of 1.8 mmHg (95%-CI: 0.2; 3.5) and AIx of 6.3% (95%-CI: 1.1; 11.5) only after exposure to CB. No significant effect was seen for the PWA surrogates AP and AIx for TB and FS, even though a slight increase in point estimates occurred directly after exposure (Fig. 1)".

When investigating the effect of different particle metrics within each exposure, we observed distinct differences in the pattern of response (Fig. 2). For CB and FS, we observed effects of primarily fine and ultrafine particles as shown by clear increases in AIx (Fig. 2) and AP (Fig. A.1) for UFP (CB and FS) and for PSC (FS only). Within the fraction of UFP, the smallest particles (< 30 nm) were responsible for the effect of CB and the fraction of particles between 30 and 100 nm dominated the effect of FS. The effects of PNC from CB were immediate, reaching a maximum directly after the exposure, becoming smaller after 2 and 4 h after the exposure and were no longer detectable after 24 h. The effects of PNC from FS were also immediate but persisted up to 24 h. After the exposure to TB primarily the larger particles (PM_{10} and $PM_{2.5}$) led to noticeably increases in AIx (Fig. 2). These effects of PM_{10} and $PM_{2.5}$ from TB reached a peak directly and 2 h after exposure and returned to pre-exposure values after 4 h and 24 h (Fig. 2).

In two-pollutant models, the effects of UFPs on AIx and less strongly on AP measured during CB and FS increased upon adjustment with PM10 for nearly all size fractions and time points (Fig. A.2; Fig. A.3). When adjusting for UFPs the effects of PM_{10}, $PM_{2.5}$, and PM_1 on AIx and AP did not change at all (Fig. A.4 and Fig. A.5). The observed increases

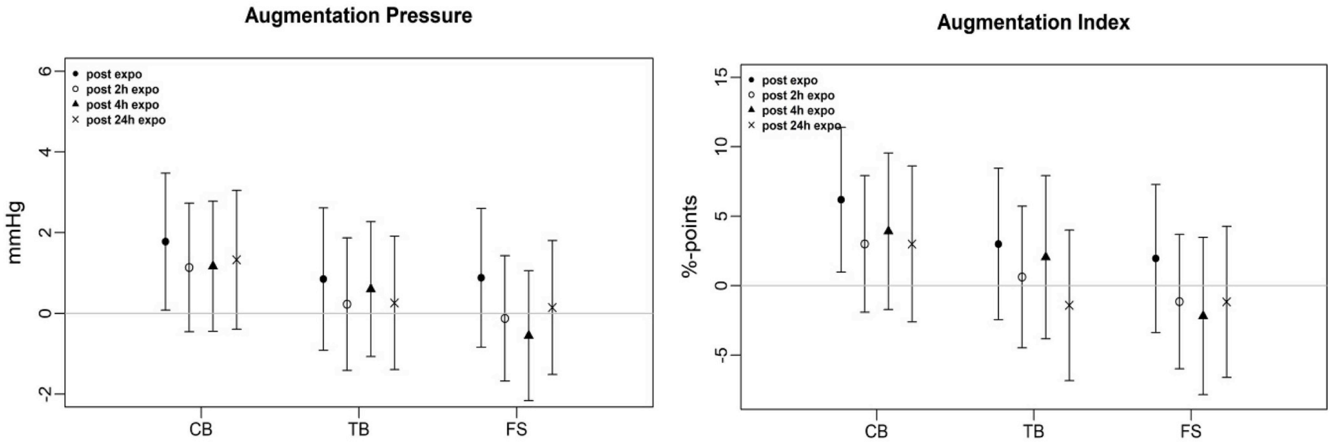

Fig. 1. Mean effect estimates and 95% Confidence Intervals (CI) for changes in augmentation pressure (AP) and augmentation index (AIx) depending on exposure (candle burning CB, toasting bread TB and frying sausages FS) in the fully adjusted model.

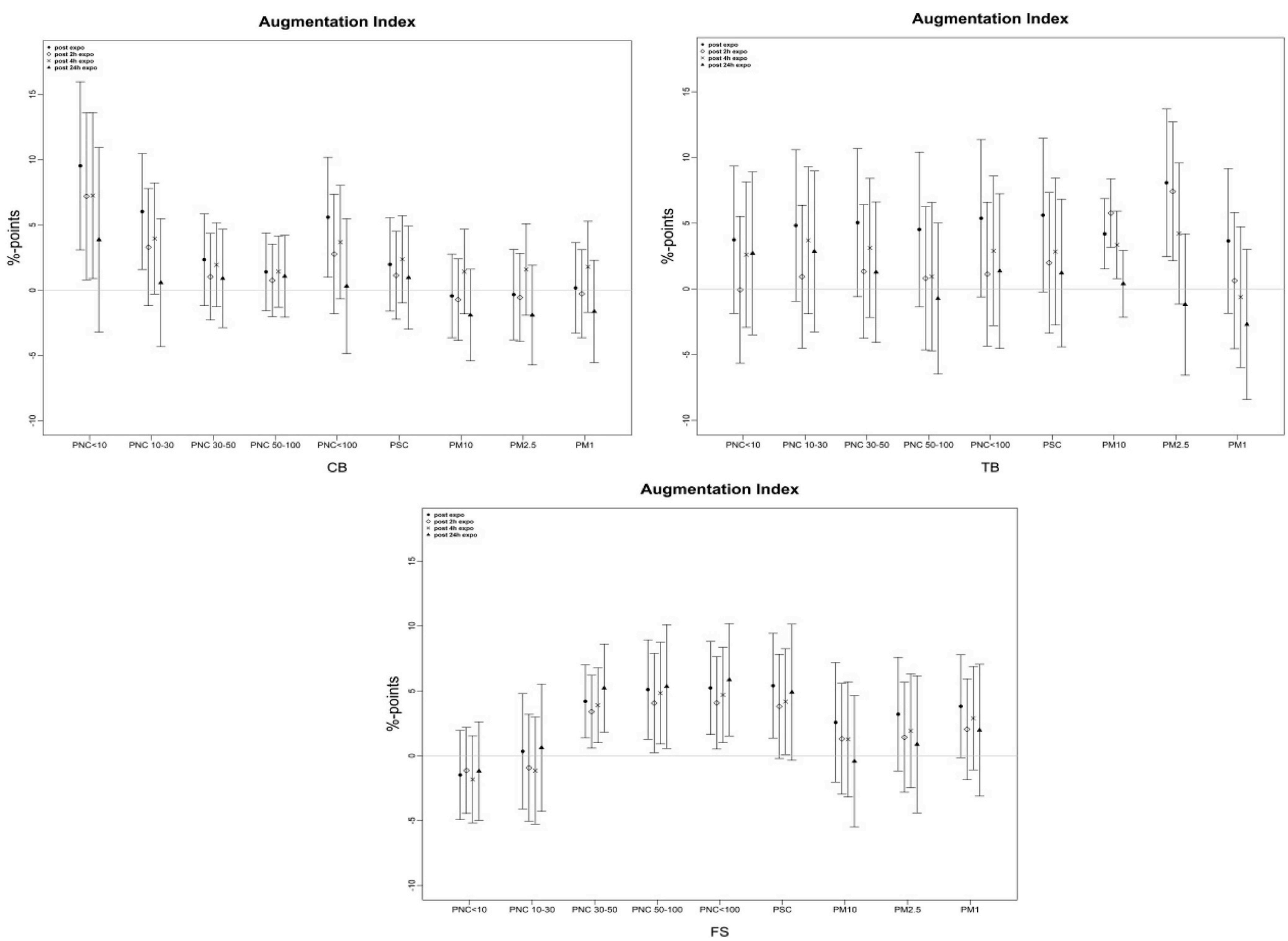

Fig. 2. Mean effect estimates and 95% confidence intervals (CI) for changes per IQR in Augmentation Index (AIx) depending on particle metric (PNC, PSC, PMC) and exposure (candle burning CB, toasting bread TB and frying sausages FS) in the fully adjusted model.

of arterial stiffness with PM_{10} and $PM_{2.5}$ measured during TB remained. The results are all shown in the appendix.

For PWV, we observed no clear associations in the categorical analysis, when comparing the exposure sources with room air (model 1) (Fig. 3).

When comparing different particle metrics (PMC, PSC, PNC) within each exposure scenario, we observed slightly elevated point estimates for different UFP size fractions from exposure to TB directly after the exposure, lasting up to 24 h, but confidence intervals were wide and included the null effect. Particle metrics measured during CB, TB and FS were not associated with PWV (Fig. 4). When adjusting for PM_{10} and PNC measured during each exposure scenario we could not observe any different effects (Fig. A.6 and Fig. A.7).

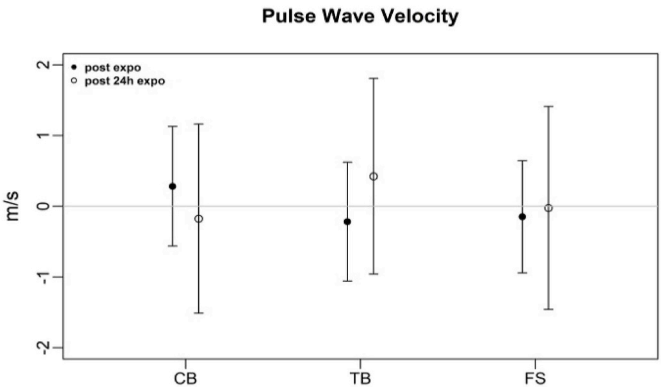

Fig. 3. Mean effect estimates and 95% Confidence Intervals (CI) for changes in pulse wave velocity (PWV) depending on exposure scenario (candle burning CB, toasting bread TB and frying sausages FS) in the fully adjusted model.

5. Discussion

In this controlled exposure study, we investigated fine and ultrafine particle emissions from specific indoor activities and their impact on arterial stiffness in healthy adults. Our study results show immediate and mostly transient effects on arterial stiffness indices depending on the exposure source and particle metric.

We observed that short-term exposure to indoor sources (CB, TB and FS) of fine and ultrafine particles leads to rapid increases in arterial stiffness. These changes of central arterial indices differ concerning magnitude, duration, and association depending on the particle metric. Most associations could be observed for PNC measured during FS and CB and arterial stiffness, in which the strongest and most lasting effects (up to 24 h after the exposure) were detected for UFPs from FS, mainly caused by particles between 30 and 100 nm. This is in accordance with the fact that UFPs (< 100 nm) measured during FS are dominated by particles between 30 and 100 nm of size (Table 2). In contrast, the observed clear effects of PNC of UFPs from CB are mainly due to particles smaller than 10 nm and partly by particles between 10 and 30 nm, which is also the dominating size fraction for UFPs from CB. The overall clear effect of UFPs from typical indoor sources on arterial stiffness are in line with current evidence for ambient UFP, showing that UFP exposures have a measureable impact on the cardiovascular system (Health Effect Institute, 2013; Weichenthal et al., 2011; Ohlwein et al., 2019). Controlled exposure and real-world studies show that UFP emissions can lead to altered endothelial function, and increased markers of inflammation (Health Effect Institute, 2013; Ohlwein et al., 2019). Inflammation is one underlying risk factor for endothelial dysfunction and resulting arterial stiffness (Jain et al., 2014).

Although mass concentration measured during TB was considerably lower than during FS, effects of PMC on arterial stiffness could only be observed for TB. A possible explanation could be that not only physical characteristics but also chemical composition of particles are responsible for increases in arterial stiffness. PMC from TB included soot particles, which have been shown to be related to vascular function before (Hoffmann et al., 2012).

While we observed distinct patterns of association of various particle size fractions with AIx and AP, we did not observe significant associations with PWV. This absence of significant associations is not an evidence for no association. But it could also be that there is no

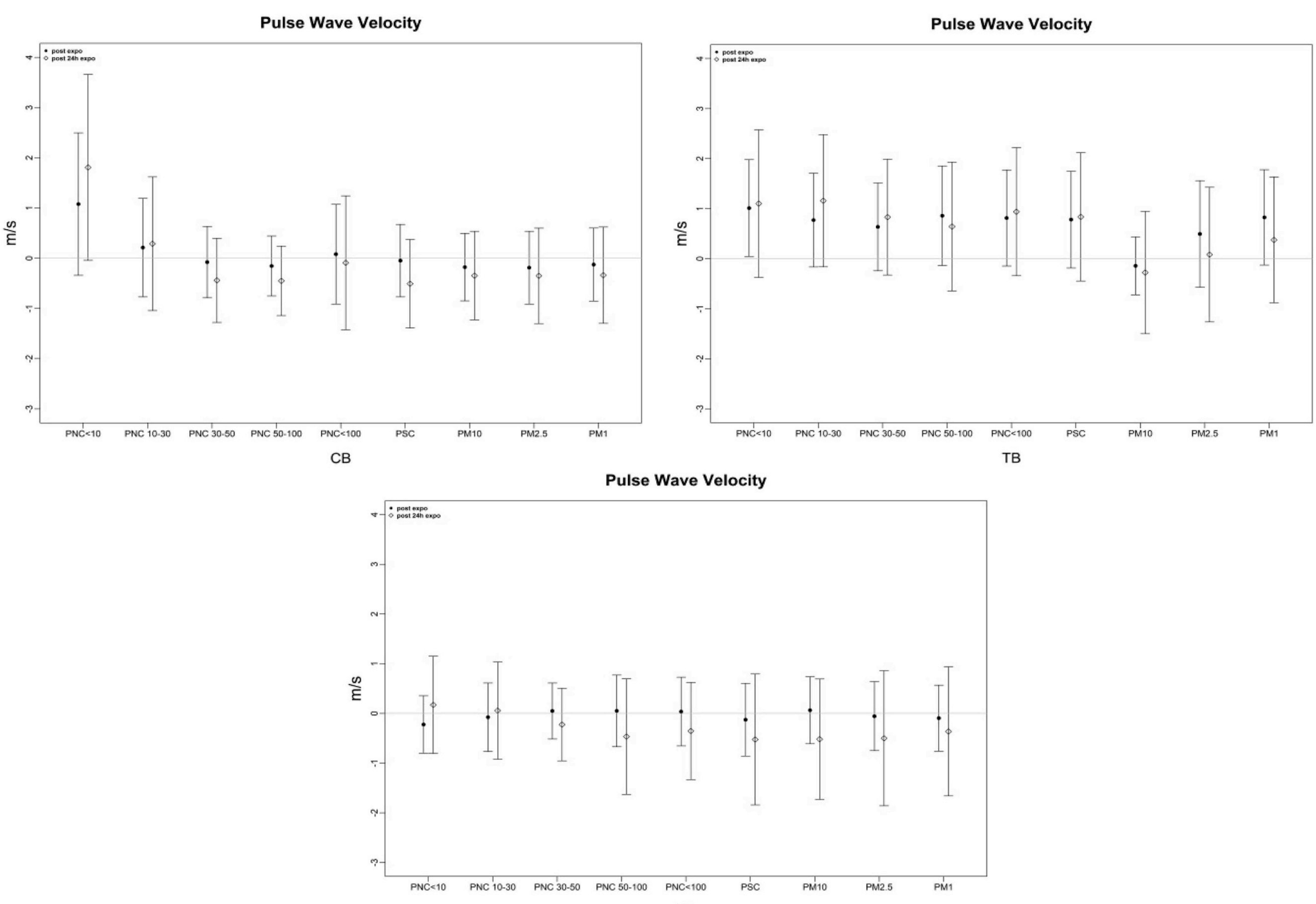

Fig. 4. Mean effect estimates and 95% confidence intervals (CI) for changes per IQR in pulse wave velocity (PWV) depending on particle metric (PNC, PSC, PMC) and exposure (candle burning CB, toasting bread TB and frying sausages FS) in the fully adjusted model.

association and that this is caused by the relatively young age (32.5 ± 16.3 years) of the study population. Present data suggest that the AIx might be a more sensitive marker of arterial stiffness in younger individuals (< 50 years), whereas PWV seems to be a better measure in older individuals (> 50 years) (McEniery et al., 2005). It is hypothesized that with growing age elastin fatigue fracture and degradation increases, with a consequent enlarged loading on stiffer collagen fibers (McEniery et al., 2005) and increases in PWV. Additionally, the increase in calcification of arteries with age might also contribute to a loss of arterial distensibility, which is also related to PWV but not that strong to AIx and AP (McEniery et al., 2005; Palatini et al., 2011). Our findings that indoor air pollution leads to changes in cardiovascular function are in line with the studies of Baumgartner et al. (2018) and Pratali et al., (2019), showing that household air pollution (indoor $PM_{2.5}$) was associated with elevated blood pressure, and with increased AIx (not significant), but not associated with PWV (Baumgartner et al., 2018). Moreover, indoor air pollution (PM_{10}, $PM_{2.5}$ and black carbon) in Nepal was negatively associated with lung function and cardiovascular function (Pratali et al., 2019).

The particle emissions from CB, TB and FS, which we produced in our study, were relatively high compared to everyday life. However, even in routine situations at home, insufficient ventilation can potentially lead to relevant personal cumulative exposures to fine and ultrafine particles indoors, if strong indoor sources are active, like cooking on several cooktops, open fireplaces, cigarette smoke. In our study, the highest mean PMC was observed during FS with 210 μg/m^3 PM_{10} and 169 μg/m^3 $PM_{2.5}$, the latter thus being two-thirds lower than the maximum mean $PM_{2.5}$ concentration measured in residential houses in Brisbane, Australia, during cooking sessions (535 μg/m^3 $PM_{2.5}$) (Morawska et al., 2003). It can therefore be assumed that particle concentrations as high as produced in our study may also occur indoors in real life.

We observed slightly different temporal patterns with on the one hand rapid and transient increases (within minutes to hours), and subacute increases (within hours to days) of arterial stiffness indices. The rapid increases in arterial stiffness after short term exposure to indoor air pollution are in line with the observations described in a review from Langrish et al. (2012), linking short term air pollution to acute effects on the arterial system, blood pressure, myocardial ischemia and induced cardiac arrhythmias (Langrish et al., 2012). In another review from Weichenthal et al. (2011) similar results could be shown for the effects of UFPs and changes in the autonomic nervous system, myocardial substrate and myocardial vulnerability (Weichenthal et al., 2011). Since these effects occur very rapidly after the exposure to particulate matter, it has been suggested that the effects are probably driven by a particle-induced activation of the autonomic nervous system (Langrish et al., 2012). One possible pathway is the activation of receptors and nerve endings in human airways, that after stimulation by inhaled PM may be capable of altering ANS pathways leading to a blunting of CV parasympathetic tone and a relative favoring of sympathetic activity (Widdicombe and Lee, 2001). The rapid and transient increases of AIx HR75 and AP HR75 after the exposure TB and CB support the previous evidence and therefore might be a result of activation of these reflex arches.

The effects of exposure to FS on arterial stiffness were more subacute and could be observed until 24 h. Regarding the short exposure duration of 2 h this effect may not solely be attributed to an imbalance of the autonomic nervous system. This ongoing increase in arterial stiffness after particle exposure could be a consequence of inflammation, in which the pro-inflammatory or oxidative stress mediators are generated in the lungs and released into the systemic circulation. The systemic spill-over of lung cell-derived cytokines causing inflammation and oxidative stress is linked to atherosclerosis, vascular dysfunction, arterial stiffness and hypertension (Franklin et al., 2015).

Clear associations of PSC and arterial stiffness were only observed for FS and, to a lesser extent, for TB, but not for CB. In addition, despite lower PMC measured during TB than during FS, we detected significant effects of PMC from TB on arterial stiffness. One explanation for these findings could be different source-specific constituents of the different emissions, resulting in different toxicity. Toxicological investigations have indeed demonstrated that, depending on their chemical composition and source, the toxic potency of PM samples of similar size fractions can vary considerably (Schaumann et al., 2004; Schins et al., 2004; Steenhof et al., 2011; Wessels et al., 2008). In a review from Schwarze et al., 2006 it is postulated that chemical characteristics of PM are important for adverse health effects.

Our study has several limitations. Due to sick leave and premature discontinuity not all participants received all exposure scenarios. Although we endeavored to choose exposure scenarios reflecting everyday use as closely as possible, there were some differences to real life situations such as the replacement of candles before burning down and FS in a pan without fat. This was done to decrease additional emissions from soot and burning fat. One major limitation was that the participants could not be blinded to the type of exposure so that they could see and smell it. Therefore we cannot exclude an additional effect of odor. Due to the small sample size, it is possible that the power for detecting cardiovascular effects may have been too low. Another limitation of this study is the possibility to have chance findings due to multiple testing. Though this is counterbalanced by the advantage of investigating several different exposure metrics and exposure times, yielding the opportunity to look for patterns throughout. Only if these patterns indicate an association, then we interpreted this as such. The strengths of our study are that we had a detailed exposure characterization with UFPs measured in different size fractions, so that an accurate assignment to different particle sizes of UFP-effects on arterial stiffness was possible. Our study design included repeated exposures so that the inter-individual variability was reduced. Another strength of the study is that we were able to additionally control for ambient air pollution received prior to the study center visit.

6. Conclusions

Our study shows immediate and mostly transient effects of indoor exposure to fine and ultrafine particles on systemic arterial stiffness indices that depend on the indoor source as well as on particle metric. Differences in size- and source-specific particles might account for these differential associations. Number concentration of UFPs has strongest effects on arterial stiffness, whereby different particle size fractions of UFPs, according to the exposure scenario, are responsible for this effect. We did not observe clear and stable associations of indoor particle exposure and PWV.

Disclaimer

The opinions expressed in this paper are those of the authors and do not necessarily reflect the views of the Federal Environmental Agency of Germany.

Ethical approval

Ethical approval for this study was received from the Ethics Committee of the Heinrich Heine University of Düsseldorf, Germany, in accordance with the declaration of Helsinki. The study registration number is: 3830.

Funding source

Funding support for this study was provided by the Federal Environmental Agency of Germany (FKZ 371162205).

Informed consent

Informed consent was obtained from all study participants.

Author contributions

Vanessa J. Soppa coordinated the field work, analyzed and interpreted data, and drafted the manuscript. Roel P. F. Schins designed the study, interpreted data and revised the manuscript. Frauke Hennig provided statistical support, interpreted data and revised the manuscript. Bryan Hellack conducted field work, performed particle measurements, analyzed and interpreted measurement data, and revised the manuscript. Ulrich Quass designed the study, performed particle measurements, analyzed and interpreted measurement data, and revised the manuscript. Heinz Kaminski performed all particle measurements, analyzed and interpreted measurement data, and revised the manuscript. Birgitta Sasse and Samir Shinnawi conducted the field study and helped in evaluating data. Thomas A. J. Kuhlbusch designed the study, discussed and interpreted the measurement and data, and revised the manuscript. Barbara Hoffmann designed the study, interpreted data and revised the manuscript.

Acknowledgements

We would like to thank our peer-researchers who facilitated recruitment, field work and the communication of study results to participants. We also thank our community partners at the IUTA.

Appendix

Table A.1

Correlation coefficient (Spearman *r*) between exposure metrics (PMC, PSC, PNC) at different exposure scenarios (room air, candle burning, toasting bread, frying sausages)

Particle metric	PMC [µg/m³]			PSC [µm²/cm³]	PNC [#/cm³]				
	PM_{10}	$PM_{2.5}$	PM_1		< 10 nm	10–30 nm	30–50 nm	50–100 nm	< 100 nm
room air (N = 34)									
PMC [µg/m³]									
PM_{10}	1								
$PM_{2.5}$	0.99	1							
PM_1	0.96	0.99	1						
PSC [µm²/cm³]	0.91	0.91	0.88	1					
PNC [#/cm³]									
< 10 nm	−0.24	−0.28	−0.31	−0.04	1				
10–30 nm	−0.16	−0.18	−0.20	0.12	0.84	1			
30–50 nm	0.13	0.12	0.07	0.80	0.05	0.26	1		
50–100 nm	0.64	0.63	0.60	0.94	−0.06	0.12	0.92	1	
< 100 nm	0.18	0.16	0.11	0.77	0.42	0.62	0.90	0.84	1
candle burning (N = 61)									
PMC [µg/m³]									
PM_{10}	1								
$PM_{2.5}$	1	1							
PM_1	0.98	0.99	1						
PSC [µm²/cm³]	0.77	0.79	0.85	1					
PNC [#/cm³]									
< 10 nm	−0.23	−0.20	−0.11	0.44	1				
10–30 nm	0.18	0.22	0.32	0.65	0.88	1			
30–50 nm	0.75	0.77	0.83	0.94	0.34	0.65	1		
50–100 nm	0.82	0.84	0.88	0.93	0.17	0.48	0.97	1	
						0,97			
< 100 nm	0.39	0.43	0.52	0.81	0.81	0.97	0.81	0.67	1
toasting bread (N = 59)									
PMC [µg/m³]									
PM_{10}	1								
$PM_{2.5}$	0.82	1							
PM_1	0.49	0.90	1						
PSC [µm²/cm³]	0.38	0.77	0.91	1					
PNC [#/cm³]									
< 10 nm	0.14	0.40	0.51	0.71	1				
10–30 nm	0.19	0.47	0.60	0.83	0.94	1			
30–50 nm	0.32	0.68	0.82	0.97	0.79	0.92	1		
50–100 nm	0.42	0.84	0.97	0.98	0.67	0.77	0.93	1	
< 100 nm	0.32	0.68	0.83	0.96	0.85	0.95	0.99	0.93	1
frying sausages (N = 64)									
PMC [µg/m³]									
PM_{10}	1								
$PM_{2.5}$	0.96	1							
PM_1	0.93	0.99	1						
PSC [µm²/cm³]	0.87	0.94	0.96	1					
PNC [#/cm³]									
< 10 nm	−0.52	−0.50	−0.51	−0.43	1				
10–30 nm	−0.43	−0.37	−0.36	−0.27	0.85	1			
30–50 nm	0.55	0.65	0.69	0.83	−0.27	0.08	1		
50–100 nm	0.84	0.91	0.93	0.96	−0.53	−0.31	0.89	1	
< 100 nm	0.71	0.80	0.83	0.92	−0.33	−0.03	0.98	0.96	1

Table A.2
IQRs for different PNC, PSC and PMC measured during CB, TB and FS

	PNC					PSC	PMC		
	< 10 nm	10–30 nm	30–50 nm	50–100 nm	< 100 nm		PM_{10}	$PM_{2.5}$	PM_1
CB	145581.60	400571.90	169005.90	93377.90	793089.60	1387.80	31.10	32.80	33.90
TB	30729.30	209001.30	213601.50	166562.00	610334.50	1835.40	53.50	51.00	45.00
FS	3953.70	41888.60	77422.30	216626.80	285746.60	2593.00	244.70	188.40	161.80

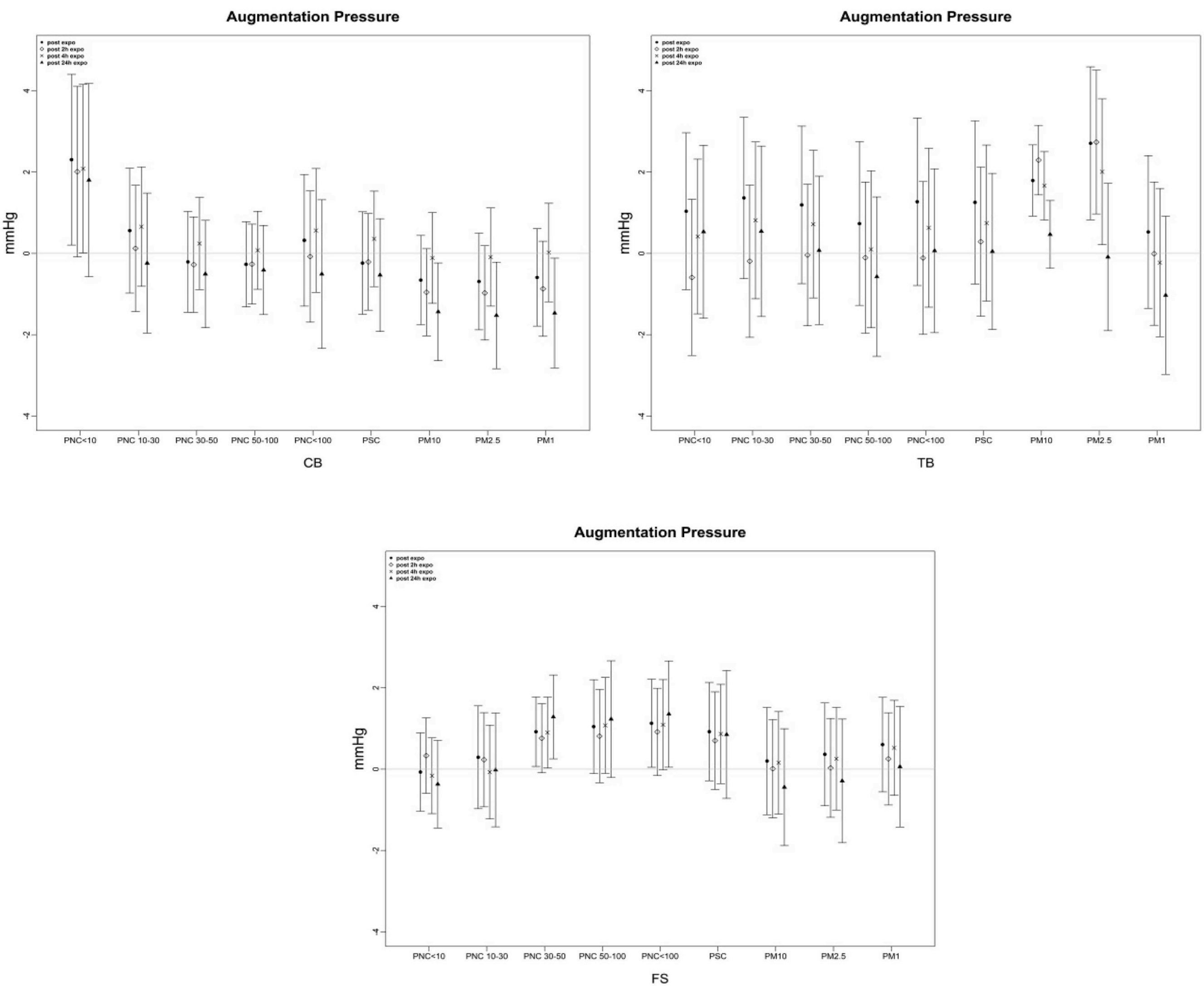

Fig. A.1. Mean effect estimates and 95% confidence intervals (CI) for changes per IQR in Augmentation Pressure (AP) depending on particle metric (PNC, PSC, PMC) and exposure (candle burning CB, toasting bread TB and frying sausages FS) in the fully adjusted model.

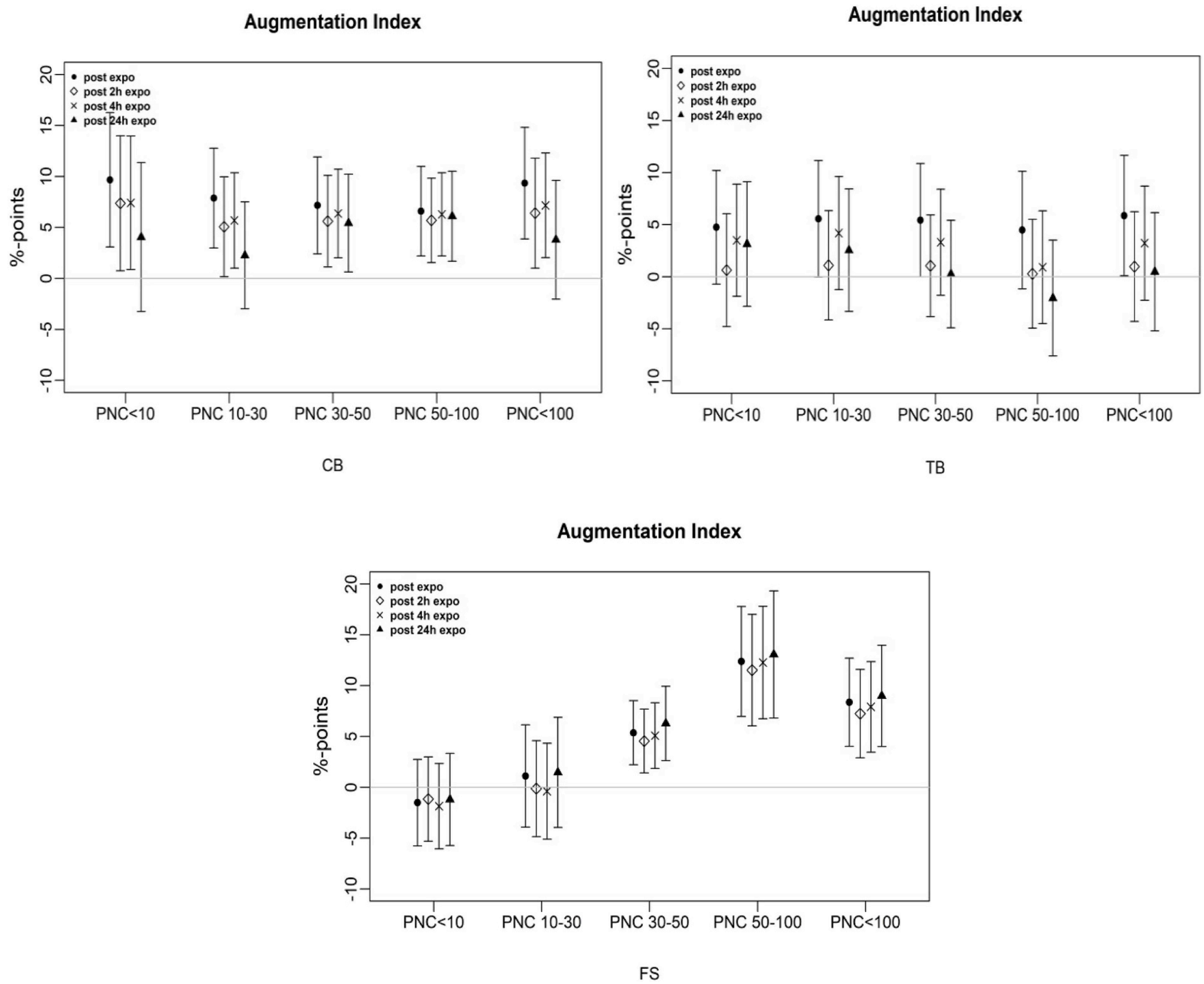

Fig. A.2. Mean effect estimates and 95% confidence intervals (CI) for changes per IQR in Augmentation Index (AIx) depending on PN size fraction (< 10 nm, 10–30 nm, 30–50 nm, 50–100 nm, < 100 nm) and exposure (candle burning CB, toasting bread TB and frying sausages FS) when adjusting additionally for PM_{10}, in the fully adjusted model.

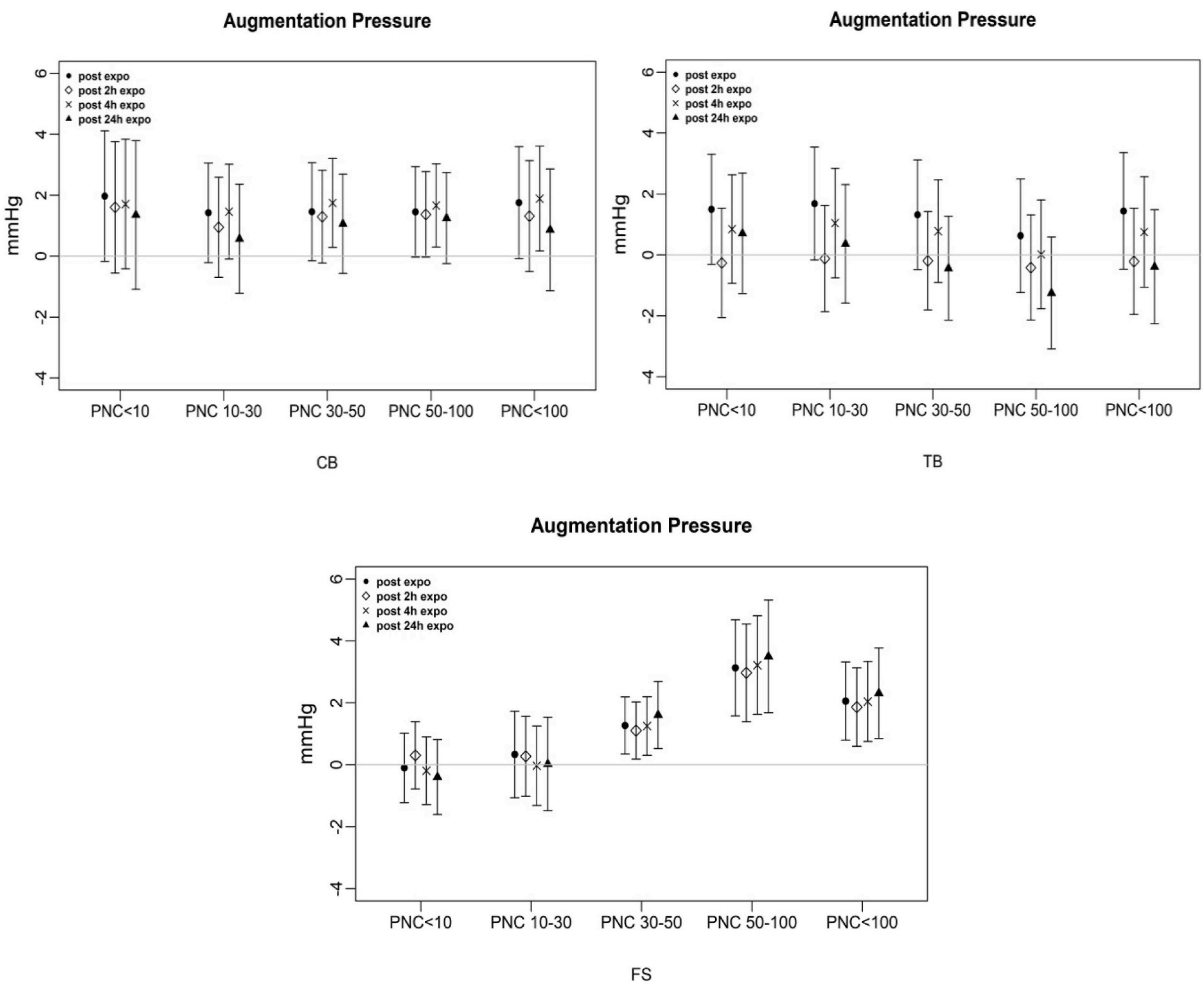

Fig. A.3. Mean effect estimates and 95% confidence intervals (CI) for changes per IQR in Augmentation Pressure (AP) depending on PN size fraction (< 10 nm, 10–30 nm, 30–50 nm, 50–100 nm, < 100 nm) and exposure (candle burning CB, toasting bread TB and frying sausages FS) when adjusting additionally for PM_{10}, in the fully adjusted model.

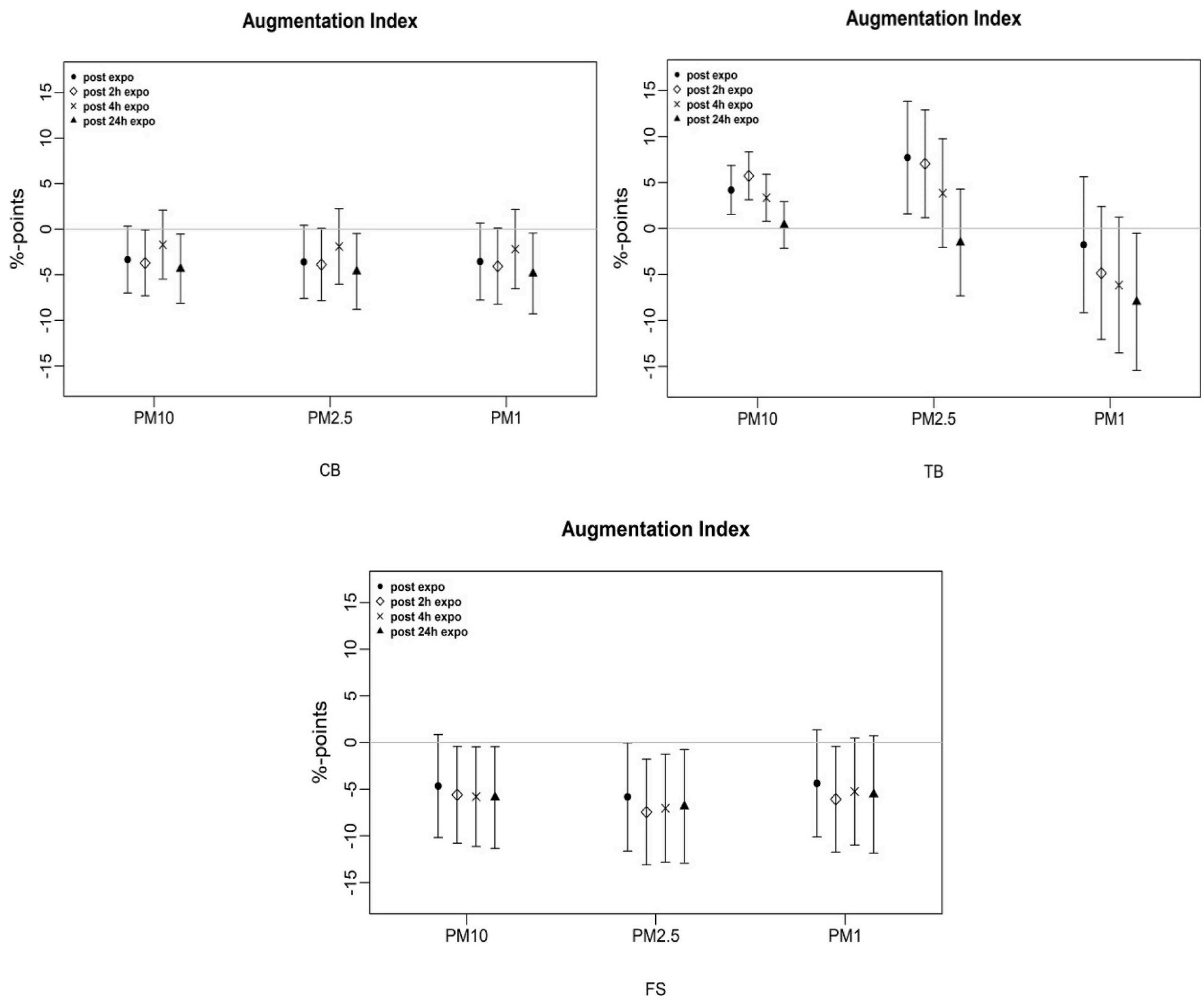

Fig. A.4. Mean effect estimates and 95% confidence intervals (CI) for changes per IQR in Augmentation Index (AIx) depending on PMC (PM_{10}, $PM_{2.5}$ and PM_1) and exposure (candle burning CB, toasting bread TB and frying sausages FS) when adjusting additionally for PNC (< 100 nm), in the fully adjusted model.

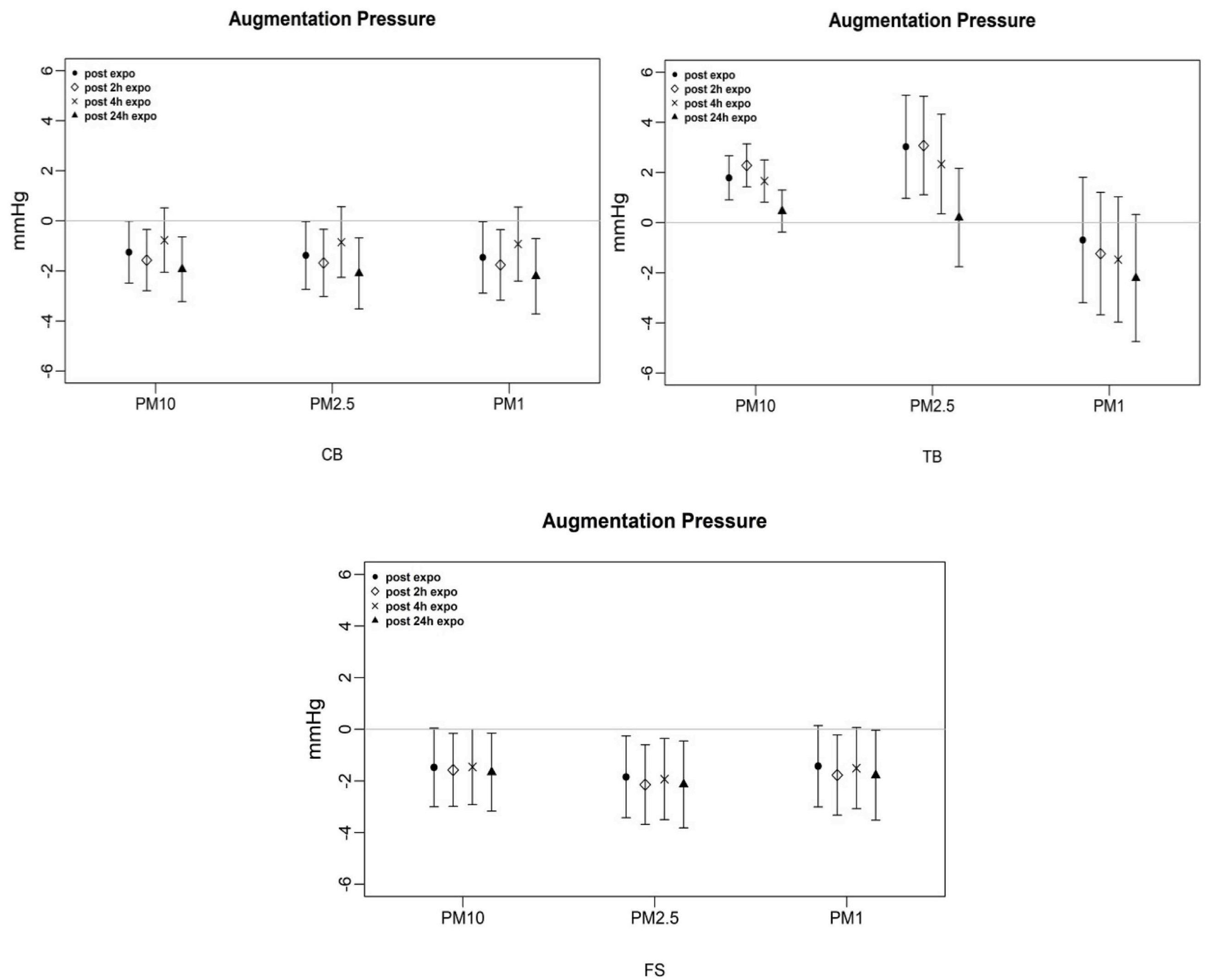

Fig. A.5. Mean effect estimates and 95% confidence intervals (CI) for changes per IQR in Augmentation Pressure (AP) depending on PMC (PM_{10}, $PM_{2.5}$ and PM_1) and exposure (candle burning CB, toasting bread TB and frying sausages FS) when adjusting additionally for PNC (< 100 nm), in the fully adjusted model.

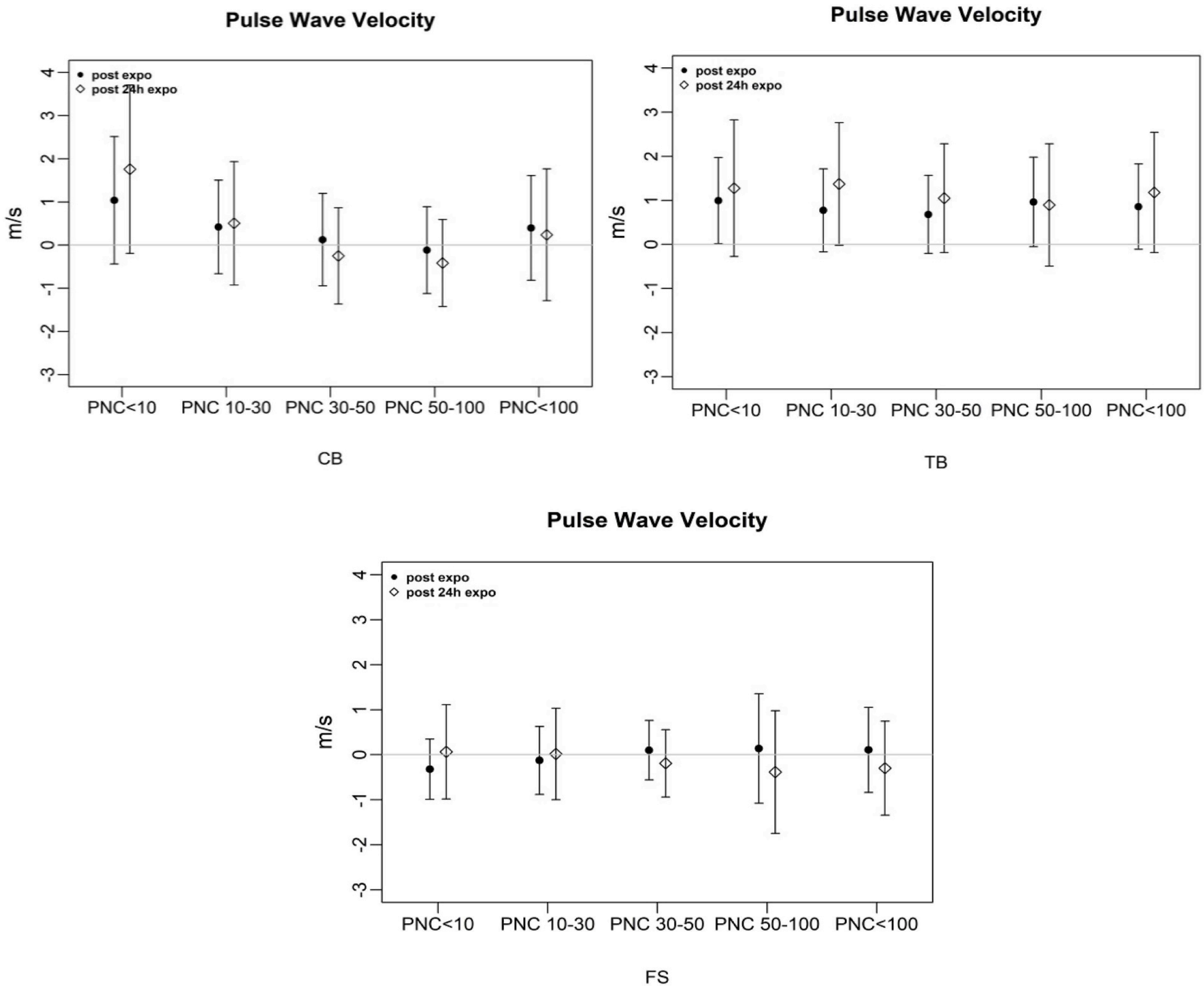

Fig. A.6. Mean effect estimates and 95% confidence intervals (CI) for changes per IQR in pulse wave velocity (PWV) depending on PN size fraction (< 10 nm, 10–30 nm, 30–50 nm, 50–100 nm, < 100 nm) and exposure (candle burning CB, toasting bread TB and frying sausages FS) when adjusting additionally for PM_{10}, measured during each exposure scenario.

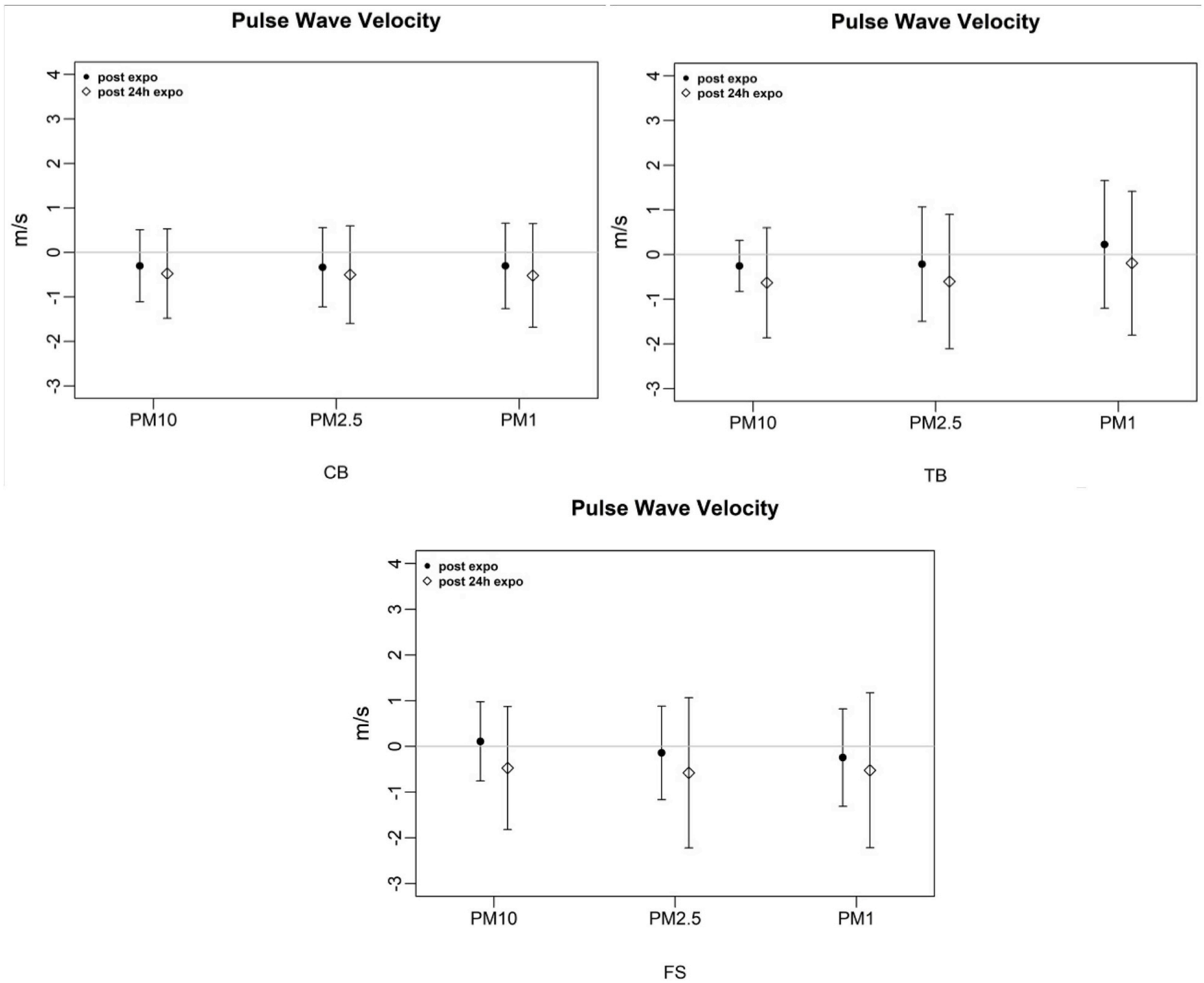

Fig. A.7. Mean effect estimates and 95% confidence intervals (CI) for changes per IQR in pulse wave velocity (PWV) depending on PMC (PM_{10}, $PM_{2.5}$ and PM_1) and exposure (candle burning CB, toasting bread TB and frying sausages FS) when adjusting additionally for PNC (< 100 nm), measured during each exposure scenario.

Table A.3
Mean effect estimates (percent points) and 95% confidence intervals (CI) for changes per IQR in Augmentation Index (AIx) depending on particle metric (PNC, PSC, PMC) and exposure (candle burning CB, toasting bread TB and frying sausages FS) in the unadjusted model.

Augmentation Index									
Time point	CB								
	PNC (#/cm^3)					PMC (µg/m^3)			PSC (µm^2/cm^3)
	< 10 nm	10–30 nm	30–50 nm	50–100 nm	< 100 nm	PM_1	$PM_{2.5}$	PM_{10}	
Post expo	1.9 (−2.6; 6.5)	2.9 (−1.1; 6.8)	2.2 (−1.3; 5.8)	1.5 (−1.5; 4.5)	3.6 (−0.9; 8.0)	0.5 (−3.0; 3.9)	0.1 (−3.4; 3.5)	0.1 (−3.2; 3.2)	2.1 (−1.6; 5.7)
Post 2 h expo	−0.7 (−4.9; 3.6)	−0.1 (−3.9; 3.7)	1.1 (−2.3; 4.4)	0.9 (−1.9; 3.7)	0.6 (−3.7; 4.9)	0.2 (−3.2; 3.6)	−0.1 (−3.4; 3.4)	−0.2 (−3.3; 2.9)	1.3 (−2.1; 4.7)
Post 4 h expo	−1.1 (−5.3; 3.1)	0.1 (−3.5; 3.8)	1.8 (−1.5; 5.0)	1.6 (−1.2; 4.3)	1.0 (−3.1; 5.1)	2.2 (−1.4; 5.7)	2.1 (−1.5; 5.6)	1.9 (−1.3; 5.2)	2.5 (−0.9; 5.9)
Post 24 h expo	−5.0 (−10.1; 0.1)	−3.3 (−7.5; 0.9)	0.9 (−2.7; 4.6)	1.4 (−1.6; 4.4)	−2.2 (−6.9; 2.5)	−0.5 (−4.3; 3.3)	−0.8 (−4.5; 2.9)	−0.8 (−4.3; 2.6)	1.5 (−2.3; 5.2)
TB									
Post expo	2.2 (−3.3; 7.6)	2.9 (−2.8; 8.6)	2.1 (−3.2; 7.5)	1.6 (−3.6; 6.8)	2.6 (−3.2; 8.3)	1.3 (−3.4; 6.1)	2.8 (−1.9; 7.7)	1.7 (−0.7; 4.2)	2.3 (−3.1; 7.7)
Post 2 h expo	−1.6 (−7.1; 3.9)	−1 (−6.4; 4.4)	−1.3 (−6.0; 3.5)	−1.9 (−6.6; 2.9)	−1.5 (−6.7; 3.7)	−1.6 (−6.0; 2.8)	2.6 (−2.0; 7.2)	3.5 (1.1; 5.9)	−1.1 (−5.9; 3.8)
Post 4 h expo	0.8 (−4.6; 6.2)	1.7 (−3.9; 7.2)	0.4 (−4.7; 5.4)	−2.2 (−7.1; 2.8)	0.1 (−5.4; 5.5)	−3.3 (−7.9; 1.3)	−0.6 (−5.3; 4.0)	1.5 (−0.9; 3.9)	−0.6 (−5.7; 4.5)
Post 24 h expo	1.5 (−4.1; 7.2)	1.4 (−4.2; 6.9)	−0.1 (−4.8; 4.6)	−1.7 (−6.5; 3.1)	−0.1 (−5.2; 5.1)	−2.9 (−7.7; 1.9)	−2.8 (−7.7; 2.1)	−0.7 (−3.2; 1.8)	−0.6 (−5.4; 4.2)
FS									
Post expo	−2.3 (−5.6; 1.1)	−0.4 (−5.0; 4.2)	4.2 (1.5; 6.8)	5.3 (1.7; 8.8)	5.3 (1.9; 8.6)	4.4 (0.8; 8.0)	4.2 (0.3; 8.2)	4.1 (−0.2; 8.4)	5.7 (1.9; 9.5)
Post 2 h expo	−1.6 (−4.9; 1.6)	−1.4 (−5.7; 2.9)	3.4 (0.8; 6.0)	4.4 (0.8; 7.9)	4.2 (0.9; 7.5)	2.8 (−0.7; 6.4)	2.7 (−1.1; 6.5)	2.9 (−0.9; 6.9)	4.3 (0.6; 7.9)
Post 4 h expo	−2.3 (−5.6; 0.9)	−1.6 (−5.9; 2.8)	3.9 (1.2; 6.6)	4.9 (1.3; 8.7)	4.7 (1.3; 8.2)	3.4 (−0.3; 7.0)	2.8 (−1.2; 6.8)	2.5 (−1.7; 6.6)	4.4 (0.6; 8.3)
Post 24 h expo	−2.1 (−5.8; 1.6)	−0.3 (−5.3; 4.8)	4.8 (1.8; 7.9)	5.9 (1.7; 10.3)	5.9 (1.9; 9.7)	4.7 (0.0; 9.4)	4.4 (−0.4; 9.2)	3.6 (−1.1; 8.2)	6.3 (1.6; 11.0)

References

Afshari, A., Matson, U., Ekberg, L.E., 2005. Characterization of indoor sources of fine and ultrafine particles: a study conducted in a full-scale chamber. Indoor Air 15, 141–150. https://doi.org/10.1111/j.1600-0668.2005.00332.x.

Baulmann, J., Weber, T., Mortensen K, et al., 2010. Messmethoden der Arteriellen Gefäßsteifigkeit. Austrian Journal of Hypertension 14 (2), 18–24.

Baumgartner, J., Carter, E., Schauer, J.J., Ezzati, M., Daskalopoulou, S.S., Valois, M.F., Shan, M., Yang, X., 2018. Household air pollution and measures of blood pressure, arterial stiffness and central haemodynamics. Heart. https://doi.org/10.1136/heartjnl-2017-312595.

Brasche, S., Bischof, W., 2005. Daily time spent indoors in German homes - baseline data for the assessment of indoor exposure of German occupants. Int. J. Hyg Environ. Health 208, 247–253. https://doi.org/10.1016/j.ijheh.2005.03.003.

Brook, R.D., Rajagopalan, S., Pope, C.A., Brook, J.R., Bhatnagar, A., Diez-Roux, A.V., Holguin, F., Hong, Y., Luepker, R.V., Mittleman, M.A., Peters, A., Siscovick, D., Smith, S.C., Whitsel, L., Kaufman, J.D., 2010. Particulate matter air pollution and cardiovascular disease: an update to the scientific statement from the american heart association. Circulation 121, 2331–2378. https://doi.org/10.1161/CIR.0b013e3181dbece1.

Brown, D.M., Wilson, M.R., MacNee, W., Stone, V., Donaldson, K., 2001. Size-dependent proinflammatory effects of ultrafine polystyrene particles: a role for surface area and oxidative stress in the enhanced activity of ultrafines. Toxicol. Appl. Pharmacol. 175, 191–199. https://doi.org/10.1006/taap.2001.9240.

Cesaroni, G., Forastiere, F., Stafoggia, M., Andersen, Z.J., Badaloni, C., Beelen, R., Caracciolo, B., de Faire, U., Erbel, R., Eriksen, K.T., Fratiglioni, L., Galassi, C., Hampel, R., Heier, M., Hennig, F., Hilding, A., Hoffmann, B., Houthuijs, D., Jöckel, K.-H., Korek, M., Lanki, T., Leander, K., Magnusson, P.K.E., Migliore, E., Ostenson, C.-G., Overvad, K., Pedersen, N.L., J, J.P., Penell, J., Pershagen, G., Pyko, A., Raaschou-Nielsen, O., Ranzi, A., Ricceri, F., Sacerdote, C., Salomaa, V., Swart, W., Turunen, A.W., Vineis, P., Weinmayr, G., Wolf, K., de Hoogh, K., Hoek, G., Brunekreef, B., Peters, A., 2014. Long term exposure to ambient air pollution and incidence of acute coronary events: prospective cohort study and meta-analysis in 11 European cohorts from the ESCAPE Project. BMJ 348, f7412. https://doi.org/10.1136/bmj.f7412.

Cruickshank, K., Riste, L., Anderson, S.G., Wright, J.S., Dunn, G., Gosling, R.G., 2002. Aortic pulse-wave velocity and its relationship to mortality in diabetes and glucose intolerance: an integrated index of vascular function? Circulation 106, 2085–2090. https://doi.org/10.1161/01.CIR.0000033824.02722.F7.

Franklin, B.A., Brook, R., Arden Pope, C., 2015. Air pollution and cardiovascular disease. Curr. Probl. Cardiol. 40, 207–238. https://doi.org/10.1016/j.cpcardiol.2015.01.003.

Ghio, A.J., Soukup, J.M., Case, M., Dailey, L. a, Richards, J., Berntsen, J., Devlin, R.B., Stone, S., Rappold, A., 2012. Exposure to wood smoke particles produces inflammation in healthy volunteers. Occup. Environ. Med. 69, 170–175. https://doi.org/10.1136/oem.2011.065276.

Health Effect Institute, 2013. Understanding the health effects of ambient ultrafine particles. HEI Perspectives 3.

HEI Review Panel on Ultrafine Particles, 2013. Understanding the health effects of ambient ultrafine particles. Heal. Eff. Inst. 122.

Hoffmann, B., Luttmann-Gibson, H., Cohen, A., Zanobetti, A., de Souza, C., Foley, C., Suh, H., Coull, B., Schwartz, J., Mittleman, M., Stone, P., Horton, E., Gold, D., 2012. Opposing effects of particle pollution, ozone, and ambient temperature on arterial blood pressure. Environ. Health Perspect. 120, 241–246. https://doi.org/10.1289/ehp.1103647.

Jain, S., Khera, R., Corrales-Medina, V.F., Townsend, R.R., Chirinos, J.A., 2014. Inflammation and arterial stiffness in humans. Atherosclerosis. https://doi.org/10.1016/j.atherosclerosis.2014.09.011.

Kapp, N., Kreyling, W., Schulz, H., Im Hof, V., Gehr, P., Semmler, M., Geiser, M., 2004. Electron energy loss spectroscopy for analysis of inhaled ultrafine particles in rat lungs. Microsc. Res. Tech. https://doi.org/10.1002/jemt.20044.

Karner, A.A., Eisinger, D.S., Niemeier, D.A., 2010. Near-roadway air quality: synthesizing the findings from real-world data. Environ. Sci. Technol. 44, 5334–5344. https://doi.org/10.1021/es100008x.

Langrish, J.P., Bosson, J., Unosson, J., Muala, A., Newby, D.E., Mills, N.L., Blomberg, A., Sandström, T., 2012. Cardiovascular effects of particulate air pollution exposure: time course and underlying mechanisms. J. Intern. Med. https://doi.org/10.1111/j.1365-2796.2012.02566.x.

Laurent, S., Boutouyrie, P., Asmar, R., Gautier, I., Laloux, B., Guize, L., Ducimetiere, P., Benetos, A., 2001. Aortic stiffness is an independent predictor of all-cause and cardiovascular mortality in hypertensive patients. Hypertension 37, 1236–1241. https://doi.org/10.1161/01.HYP.37.5.1236.

Li, N., Sioutas, C., Cho, A., Schmitz, D., Misra, C., Sempf, J., Wang, M., Oberley, T., Froines, J., Nel, A., 2003. Ultrafine particulate pollutants induce oxidative stress and mitochondrial damage. Environ. Health Perspect. 111, 455–460. https://doi.org/10.1289/ehp.6000.

Lim, Stephen S., Vos, Theo, Flaxman, Abraham D., Goodarz Danaei, K.S., Heather, Adair-Rohani, Markus, Amann, Anderson, H Ross, Martin Aryee, K.G.A., Charles, Atkinson, Loraine, J Bacchus, Adil, N Bahalim, Balakrishnan, K., John Balmes, S.B.-C., 2012. A comparative risk assessment of burden of disease and injury attributable to 67 risk factors and risk factor clusters in 21 regions, 1990–2010: a systematic analysis for the Global Burden of Disease Study 2010. Lancet 380, 2224–2260. https://doi.org/10.1016/S0140-6736(12)61766-8.A.

Lundback, M., Mills, N.L., Lucking, A., Barath, S., Donaldson, K., Newby, D.E., Sandstrom, T., Blomberg, A., 2009. Experimental exposure to diesel exhaust increases arterial stiffness in man. Part. Fibre Toxicol. https://doi.org/10.1186/1743-8977-6-7.

McEniery, C.M., Yasmin, Hall, I.R., Qasem, A., Wilkinson, I.B., Cockcroft, J.R., 2005. Normal vascular aging: differential effects on wave reflection and aortic pulse wave velocity - the Anglo-Cardiff Collaborative Trial (ACCT). J. Am. Coll. Cardiol. 46, 1753–1760. https://doi.org/10.1016/j.jacc.2005.07.037.

Mehta, A.J., Zanobetti, A., Koutrakis, P., Mittleman, M.A., Sparrow, D., Vokonas, P., Schwartz, J., 2014. Associations between short-term changes in air pollution and correlates of arterial stiffness: the veterans affairs normative aging study, 2007-2011. Am. J. Epidemiol. 179, 192–199. https://doi.org/10.1093/aje/kwt271.

Miller, M.R., Raftis, J.B., Langrish, J.P., McLean, S.G., Samutrtai, P., Connell, S.P., Wilson, S., Vesey, A.T., Fokkens, P.H.B., Boere, A.J.F., Krystek, P., Campbell, C.J., Hadoke, P.W.F., Donaldson, K., Cassee, F.R., Newby, D.E., Duffin, R., Mills, N.L., 2017. Inhaled nanoparticles accumulate at sites of vascular disease. ACS Nano. https://doi.org/10.1021/acsnano.6b08551.

Morawska, L., He, C., Hitchins, J., Mengersen, K., Gilbert, D., 2003. Characteristics of particle number and mass concentrations in residential houses in Brisbane, Australia. Atmos. Environ. https://doi.org/10.1016/S1352-2310(03)00566-1.

Oberdorster, G., Gelein, R.M., Ferin, J., Weiss, B., 1995. Association of particulate air pollution and acute mortality: involvement of ultrafine particles? Inhal. Toxicol. 7, 111–124. https://doi.org/10.3109/08958379509014275.

Ohlwein, S., Kappeler, R., Kutlar Joss, M., Künzli, N., Hoffmann, B., et al., 2019. Health effects of ultrafine particles: a systematic literature review update of epidemiological evidence. International Journa of Public Health 64 (4), 547–559. https://doi.org/10.1007/s00038-019-01202-7. PMID: 30790006.

Palatini, P., Casiglia, E., Gasowski, J., Głuszek, J., Jankowski, P., Narkiewicz, K., Saladini, F., Stolarz-Skrzypek, K., Tikhonoff, V., Van Bortel, L., Wojciechowska, W., Kawecka-Jaszcz, K., 2011. Arterial stiffness, central hemodynamics, and cardiovascular risk in hypertension. Vasc. Health Risk Manag. https://doi.org/10.2147/VHRM.S25270.

Pratali, L., Marinoni, A., Cogo, A., Ujka, K., Gilardoni, S., Bernardi, E., Bonasoni, P., Bruno, R.M., Bastiani, L., Vuillermoz, E., Sdringola, P., Fuzzi, S., 2019. Indoor air pollution exposure effects on lung and cardiovascular health in the High Himalayas, Nepal: an observational study. Eur. J. Intern. Med. https://doi.org/10.1016/j.ejim.2018.10.023.

Schaumann, F., Borm, P.J.A., Herbrich, A., Knoch, J., Pitz, M., Schins, R.P.F., Luettig, B., Hohlfeld, J.M., Heinrich, J., Krug, N., 2004. Metal-rich ambient particles (particulate matter 2.5) cause airway inflammation in healthy subjects. Am. J. Respir. Crit. Care Med. 170, 898–903. https://doi.org/10.1164/rccm.200403-423OC.

Schins, R.P.F., Lightbody, J.H., Borm, P.J.A., Shi, T., Donaldson, K., Stone, V., 2004. Inflammatory effects of coarse and fine particulate matter in relation to chemical and biological constituents. Toxicol. Appl. Pharmacol. 195, 1–11. https://doi.org/10.1016/j.taap.2003.10.002.

Schwarze, P.E., Ovrevik, J., Lag, M., Refsnes, M., Nafstad, P., Hetland, R.B., Dybing, E., et al., 2006. Particulate matter properties and health effects: consistency of epidemiological and toxicological studies. Human and Experimental Toxicology 25 (10), 559–579. https://doi.org/10.1177/096032706072520. PMID: 17165623.

Shoji, T., Emoto, M., Shinohara, K., Kakiya, R., Tsujimoto, Y., Kishimoto, H., Ishimura, E., Tabata, T., Nishizawa, Y., 2001. Diabetes mellitus, aortic stiffness, and cardiovascular mortality in end-stage renal disease. J. Am. Soc. Nephrol. 12, 2117–2124.

Soppa, V.J., Schins, R.P.F., Hennig, F., Hellack, B., Quass, U., Kaminski, H., Kuhlbusch, T.A.J., Hoffmann, B., Weinmayr, G., 2014. Respiratory effects of fine and ultrafine particles from indoor sources-a randomized sham-controlled exposure study of healthy volunteers. Int. J. Environ. Res. Public Health 11, 6871–6889. https://doi.org/10.3390/ijerph110706871.

Soppa, V.J., Schins, R.P.F., Hennig, F., Nieuwenhuijsen, M.J., Hellack, B., Quass, U., Kaminski, H., Sasse, B., Shinnawi, S., Kuhlbusch, T.A.J., Hoffmann, B., 2017. Arterial blood pressure responses to short-term exposure to fine and ultrafine particles from indoor sources – a randomized sham-controlled exposure study of healthy volunteers. Environ. Res. 158, 225–232. https://doi.org/10.1016/j.envres.2017.06.006.

Sørensen, M., Loft, S., Andersen, H.V., Raaschou-Nielsen, O., Skovgaard, L.T., Knudsen, L.E., Nielsen, I.V., Hertel, O., 2005. Personal exposure to PM2.5, black smoke and NO2 in Copenhagen: relationship to bedroom and outdoor concentrations covering seasonal variation. J. Expo. Anal. Environ. Epidemiol. 15, 413–422. https://doi.org/10.1038/sj.jea.7500419.

Steenhof, M., Gosens, I., Strak, M., Godri, K.J., Hoek, G., Cassee, F.R., Mudway, I.S., Kelly, F.J., Harrison, R.M., Lebret, E., Brunekreef, B., Janssen, N.A.H., Pieters, R.H.H., 2011. In vitro toxicity of particulate matter (PM) collected at different sites in The Netherlands is associated with PM composition, size fraction and oxidative potential–the RAPTES project. Part. Fibre Toxicol 8, 26. https://doi.org/10.1186/1743-8977-8-26.

Steppan, J., Barodka, V., Berkowitz, D.E., Nyhan, D., 2011. Vascular stiffness and increased pulse pressure in the aging cardiovascular system. Cardiol. Res. Pract. 1–8. https://doi.org/10.4061/2011/263585. 2011.

Unosson, J., Blomberg, A., Sandstrom, T., Muala, A., Boman, C., Nystrom, R., Westerholm, R., Mills, N.L., Newby, D.E., Langrish, J.P., Bosson, J.A., 2013. Exposure to wood smoke increases arterial stiffness and decreases heart rate variability in humans. Part. Fibre Toxicol 10, 20. https://doi.org/10.1186/1743-8977-10-20.

Veerasamy, M., Ford, G.A., Neely, D., Bagnall, A., MacGowan, G., Das, R., Kunadian, V., 2014. Association of aging, arterial stiffness, and cardiovascular disease: a review.

Cardiol. Rev. https://doi.org/10.1097/CRD.0000000000000009.
Ward, T., Noonan, C., 2008. Results of a residential indoor PM2.5 sampling program before and after a woodstove changeout. Indoor Air 18, 408–415. https://doi.org/10.1111/j.1600-0668.2008.00541.x.
Weichenthal, S., Kulka, R., Dubeau, A., Martin, C., Wang, D., Dales, R., 2011. Traffic-related air pollution and acute changes in heart rate variability and respiratory function in urban cyclists. Environ. Health Perspect. 119, 1373–1378. https://doi.org/10.1289/ehp.1003321.
Wessels, A., Birmili, W., Jermann, E., Wick, G., Albrecht, C., Harrison, R.M., Schins, R.P.F., 2008. Oxidant generation and toxicity in human A549 lung epithelial cells by size-fractionated atmospheric particles. Toxicol. Lett. 180, S206. https://doi.org/10.1016/j.toxlet.2008.06.246.
Widdicombe, J., Lee, L.Y., 2001. Airway reflexes, autonomic function, and cardiovascular responses. Environ. Health Perspect. 109 (Suppl. l), 579–584 10.1.1.276.2059.
Willum-Hansen, T., Staessen, J.A., Torp-Pedersen, C., Rasmussen, S., Thijs, L., Ibsen, H., Jeppesen, J., 2006. Prognostic value of aortic pulse wave velocity as index of arterial stiffness in the general population. Circulation 113, 664–670. https://doi.org/10.1161/CIRCULATIONAHA.105.579342.